Journal of *Marine Science and Engineering*

MDPI

Article

Controlling Effects of Complex Fault Systems on the Oil and Gas System of Buried Hills: A Case Study of Beibuwan Basin, China

Anran Li [1,2], Fanghao Xu [1,*], Guosheng Xu [1], Caiwei Fan [3], Ming Li [3], Fan Jiang [3], Xiaojun Xiong [1], Xichun Zhang [1] and Bing Xie [1]

[1] State Key Laboratory of Oil and Gas Reservoir Geology and Exploitation, Chengdu University of Technology, Chengdu 610059, China; swpu_lianran@swpu.edu.cn (A.L.); xiongxiaojun07@cdut.cn (X.X.); zhangxichun@stu.cdut.edu.cn (X.Z.); 2023020206@stu.cdut.edu.cn (B.X.)
[2] School of Art, Southwest Petroleum University, Chengdu 610500, China
[3] Zhanjiang Branch, China National Offshore Oil Corporation (CNOOC), Zhanjiang 524057, China; liming11@cnooc.com.cn (M.L.); jiangfan6@cnooc.com.cn (F.J.)
* Correspondence: xufanghao17@cdut.edu.cn

Abstract

Traps are central to petroleum exploration, where hydrocarbons accumulate during migration. Reservoirs are likewise an essential petroleum system element and serve as the primary medium for hydrocarbon storage. The buried hill is a geological formation highly favorable for reservoir development. However, the factors influencing hydrocarbon accumulation in buried hill reservoirs are highly diverse, especially in areas with complex, active fault systems. Fault systems play a dual role, both in the formation of reservoirs and in the migration of hydrocarbons. Therefore, understanding the impact of complex fault systems helps enhance the exploration success rate of buried hill traps and guide drilling deployment. In the Beibuwan Basin in the South China Sea, buried hill traps are key targets for deep-buried hydrocarbon exploration in this faulted basin. The low level of exploration and research in buried hills globally limits the understanding of hydrocarbon accumulation conditions, thereby hindering large-scale hydrocarbon exploration. By using drilling data, logging data, and seismic data, stress fields and tectonic faults were restored. There are two types of buried hills developed in the Beibuwan Basin, which were formed during the Late Ordovician-Silurian period and Permian-Triassic period, respectively. The tectonic genesis of the Late Ordovician-Silurian period buried hills belongs to magma diapirism activity, while the tectonic genesis of the Permian-Triassic period buried hills belongs to reverse thrust activity. The fault systems formed by two periods of tectonic activity were respectively altered into basement buried hills and limestone buried hills. The negative structural inversion controls the distribution and interior stratigraphic framework of the deformed Carboniferous strata in the limestone buried hill. The faults and derived fractures of the Late Ordovician-Silurian period and Permian-Triassic period promoted the diagenesis and erosion of these buried hills. The faults formed after the Permian-Triassic period are not conducive to calcite cementation, thus facilitating the preservation of the reservoir space formed earlier. The control of hydrocarbon accumulation by the fault system is reflected in two aspects: on the one hand, the early to mid-Eocene extensional faulting activity directly controlled the depositional process of lacustrine source rocks; on the other hand, the Late Eocene-Oligocene, which is closest to the hydrocarbon expulsion period, is the most effective fault activity period for connecting Eocene source rocks and buried hill reservoirs. This study contributes to understanding of the role of complex fault activity in the formation of buried hill traps within hydrocarbon-bearing basins.

check for updates

Academic Editor: Andrew D. La Croix

Received: 10 June 2025
Revised: 28 July 2025
Accepted: 29 July 2025
Published: 31 July 2025

Citation: Li, A.; Xu, F.; Xu, G.; Fan, C.; Li, M.; Jiang, F.; Xiong, X.; Zhang, X.; Xie, B. Controlling Effects of Complex Fault Systems on the Oil and Gas System of Buried Hills: A Case Study of Beibuwan Basin, China. *J. Mar. Sci. Eng.* **2025**, *13*, 1472. https://doi.org/10.3390/jmse13081472

Copyright: © 2025 by the authors. Licensee MDPI, Basel, Switzerland. This article is an open access article distributed under the terms and conditions of the Creative Commons Attribution (CC BY) license (https://creativecommons.org/licenses/by/4.0/).

Keywords: buried hill; tectonic fault; negative structural inversion; hydrocarbon accumulation; Beibuwan Basin; petroleum system analysis; South China Sea

1. Introduction

Basement rock is defined as the crystalline foundation or the sedimentary rocks that existed before the formation of the basin [1]. Buried hill refers to a paleo basement rock hill covered by later sediments, formed through tectonic movements that caused the uplift of the basement rock and subsequent sedimentary burial [2–4]. A buried hill reservoir is a type of oil and gas reservoir with a very wide distribution [3–6], which has been discovered in major oil and gas-bearing basins around the world [7–9], for example, the Precambrian basement highs in the Kansas region of North America, the Jurassic basement highs in the Maracaibo Basin of Venezuela, the Miocene basement highs in the Panon Basin of Hungary, the Archaean basement highs in the Mumbai Basin of India, and the Carboniferous basement highs in Western Siberia, Russia [10–12]. Exploration of basement rock oil and gas reservoirs worldwide has been ongoing for over 70 years, and this type of reservoir accounts for approximately 10% of global recoverable oil and gas reserves [7]. Compared to oil and gas fields primarily composed of sedimentary rock reservoirs, basement rock oil fields tend to be more numerous, geographically widespread, have larger stratigraphic spans, and are generally smaller in individual field size [6]. Within China, several basement rock oil and gas fields have been discovered in basins or areas such as Songliao, Jiayuan, Bohai Bay, the Southeast Sea Area, Qaidam, and Beibuwan [13–15].

Compared to conventional reservoirs, buried hill reservoirs primarily consist of metamorphic rocks, carbonates, and igneous rocks [5–8]. These rocks not only have well-developed dissolved pores and fractures but also exhibit strong resistance to compaction, making them less sensitive to depth changes. As a result, they are targeted in deep and ultra-deep hydrocarbon exploration [10]. Fault activity and fracture distribution play a crucial role in the formation of basement buried hill reservoirs and hydrocarbon accumulation [16–18]. However, the mechanisms by which complex fault systems control hydrocarbon enrichment in basement buried hills remain unclear. The Beibuwan Basin is a significant hydrocarbon-rich area in the South China Sea, characterized by highly complex and varied fault activity [19,20]. The basin has experienced multiple phases of tectonic stress field changes from the Paleozoic to the Mesozoic [21]. After over 40 years of exploration and development, the potential for conventional hydrocarbon resources has diminished, and exploration costs continue to rise. Therefore, discovering new types and stratigraphic layers of hydrocarbon resources has become increasingly crucial for enhancing reserves and production [22]. This basin provides an excellent case study for understanding how faults control basement oil and gas reservoirs. However, the genetic types, development characteristics, controlling factors, and distribution patterns of favorable basement reservoirs are not yet well understood. The lack of clear exploration targets has severely hindered the progress of basement oil and gas field exploration.

In this study, the stress field and the chronological sequence of tectonic faults in the Beibuwan Basin are identified. The impact of fault activities from different tectonic phases on the formation of basement highs is revealed. The influence of tectonic faults on basement reservoir formation and hydrocarbon accumulation is analyzed.

2. Geological Setting

The Beibuwan Basin is located in the South China Sea (Figure 1a), which is surrounded by the Leizhou Peninsula, Guangdong-Guangxi Uplift, and the Hainan Uplift [20]. From

the perspective of tectonic origin, this basin a is a typical faulted basin [21]. According to the tectonic pattern formed during the Paleogene extensional stage, the Beibuwan Basin is composed of three major structural units, including the northern depression zone, the Qixi Uplift, and the southern depression zone [20]. The Weixinan Sag is a second tectonic unit located in the NW Beibuwan Basin and was formed by extension during the Cenozoic era [21]. The Weixinan Sag provided sedimentary accommodation for a thick Cenozoic sediment sequence, including the Paleogene Changliu, Liushagang, Weizhou Formation, Neogene Xiayang, Jiaowei, Dengloujiao (Figure 1b) and Wanglougang Formation, and Quaternary strata [22]. The Beibuwan Basin has gone through two main tectonic stages, including the rift stage during the Paleogene and the depression stage during the Neogene Quaternary. The rifting stage deposited continental clastic rocks including the Changliu, Liushagang, and Weizhou Formation [23], while the depression stage mainly consisted of marine clastic rock construction (Figure 1b). The Liushagang Formation is mainly composed of dark mudstone and organic-rich shale, playing the role of source rock for the oil and gas system in the Beibuwan Basin (Figure 1b). The lake facies mudstone and shale from the Liushagang and Weizhou formations, along with the marine mudstone from the Neogene, together form multiple seal rock layers.

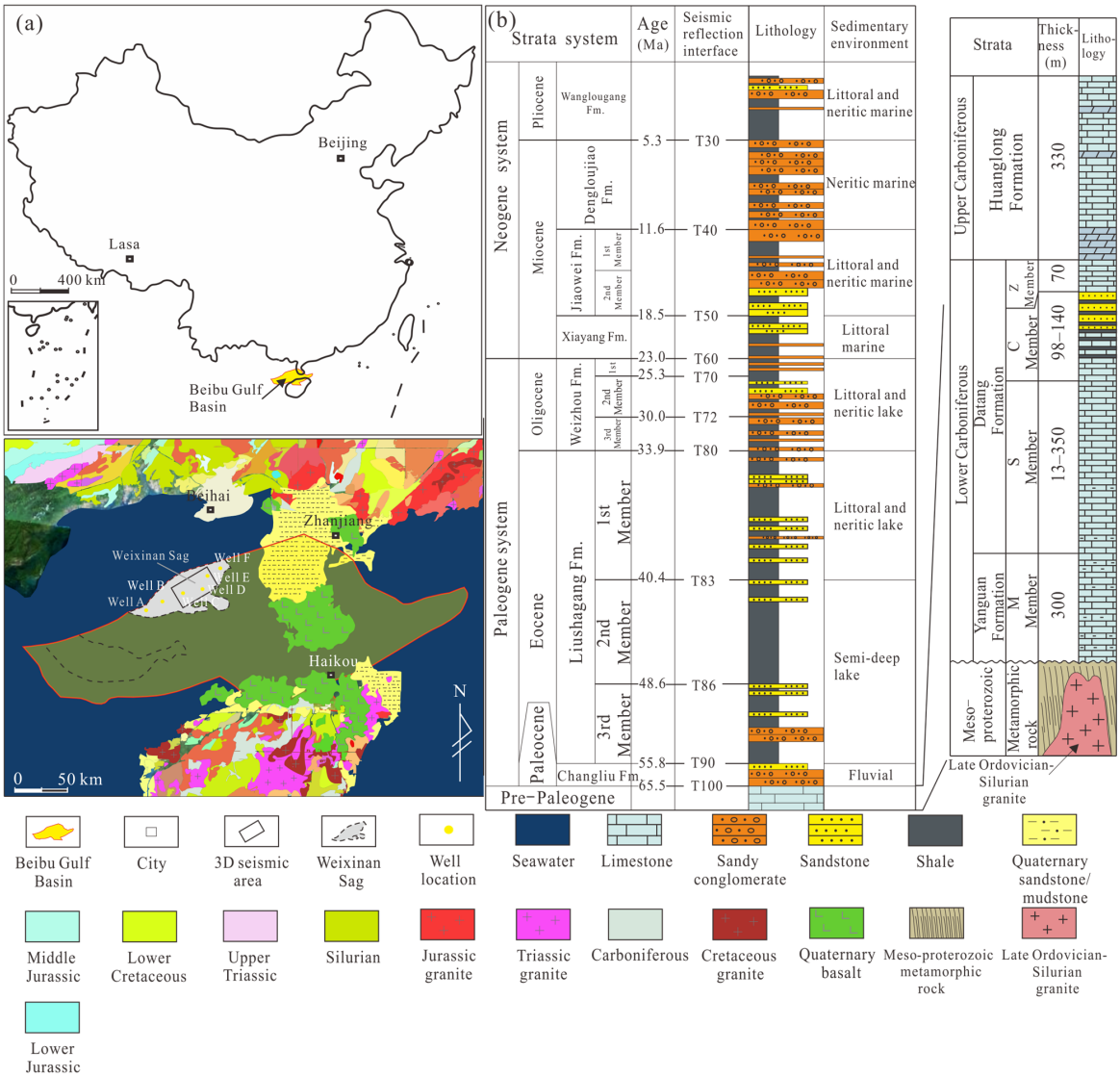

Figure 1. (**a**) Location of the Beibuwan Basin and Weixinan Sag of this study. (**b**) Generalized stratigraphy of sedimentary cover strata in the Beibuwan Basin (modified from [20]).

Since the 1960s, when China began exploring oil and gas in the South China Sea, the Beibuwan Basin has gradually become a key oil exploration and production area in the western part of the South China Sea. The discovered oil and gas reserves are distributed across several stratigraphic units, including the pre-Paleogene buried hills (Figure 2), Paleogene Liushagang and Weizhou formations, as well as the Neogene Jiaowei Formation. By 2018, the Beibuwan Basin had produced a total of approximately 4.6 million tons of crude oil [24].

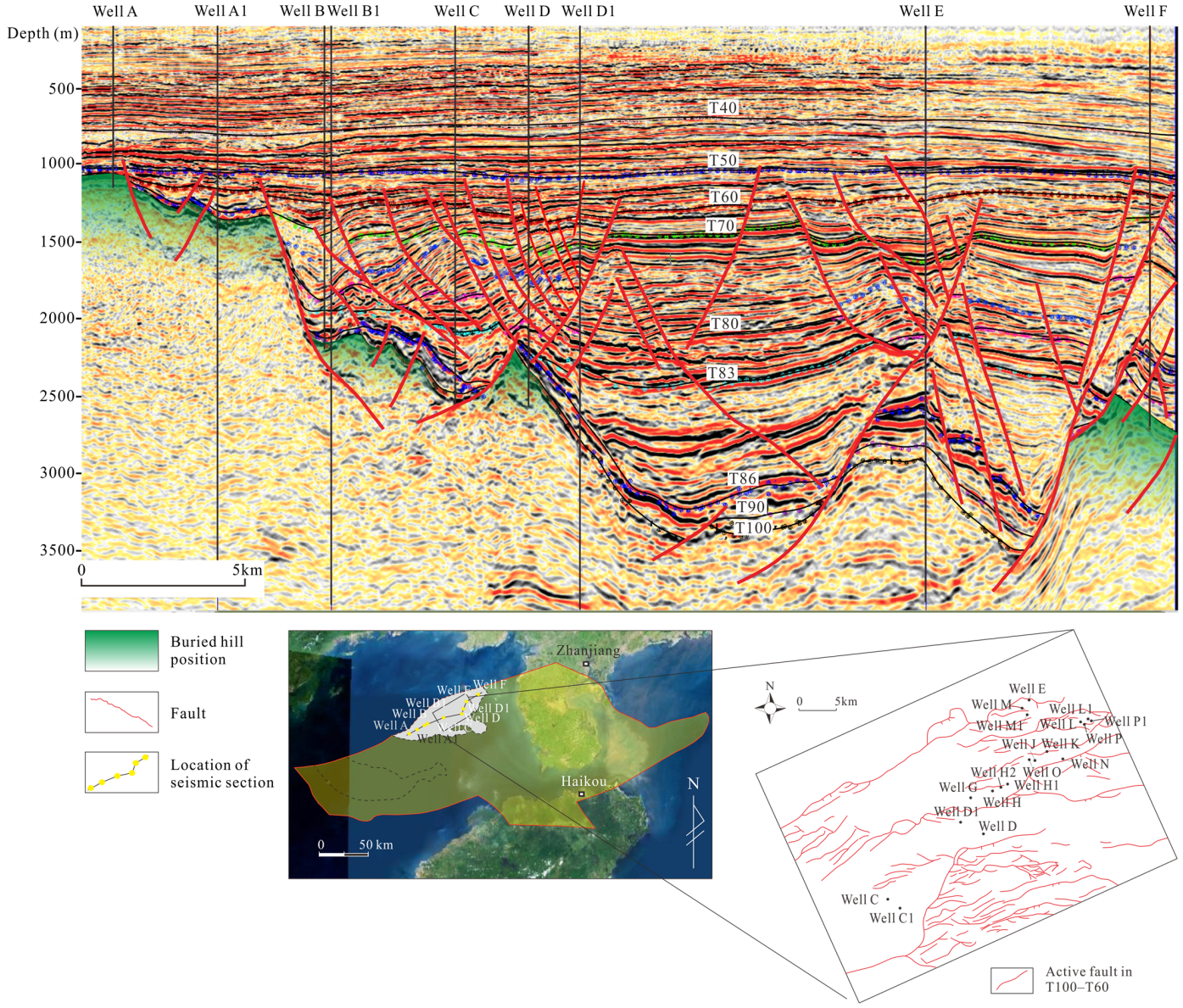

Figure 2. Cross-section of the Beibuwan Basin to show the distribution of various buried hills (section position is shown in Figure 1).

3. Samples and Methods

3.1. Seismic Data and Logging Data

The distribution of subsurface lithology revealed by 40 wells and logging data is summarized, providing a reference for subsequent analysis of lithology based on seismic response characteristics. Seven wells encountered a limestone basement, four encountered a metamorphic basement, and five encountered a granite basement. This study is mainly based on three-dimensional (3D) seismic reflection data that constrain major faults and several seismic horizons. The 3D seismic data were obtained, processed, and provided by the China National Offshore Oil Corporation (CNOOC) (Zhanjiang City, China). The data cover 300 km^2 over the study area, with an effective bandwidth of 4–26 Hz, and a main frequency of 10 Hz. The seismic trace spacing is 12.5 m × 12.5 m. The logging sequence includes sonic, resistivity, density (DEN), and natural gamma (GR) logs, among others. The 3D seismic survey included well-to-seismic calibration for 16 wells. The synthetic records are consistent with the well-log features, showing a high correlation coefficient and good matching between well and seismic data. The stratigraphic calibration results are accurate, with the top of the buried hill marked by a medium-strong peak reflection, laying the foundation for further seismic stratigraphic interpretation and layer velocity field analysis. All the logging data, including strike data and logging sequence are provided by the China National Offshore Oil Corporation (CNOOC) (Zhanjiang City, China).

3.2. Interpretation of Basement Faults

To reconstruct the formation and evolutionary patterns of the buried hills, analyzing the base faults is crucial. The original data show poor imaging quality within the buried hill, which only delineates faults with distinct offsets at the top interface, making it difficult to clearly identify and interpret internal faults. Analyzing the profile features reveals that, despite weak internal reflection energy, generally showing weak, blank, and chaotic reflections, there are several sets of steep-angle seismic reflections with some continuity inside the buried hill. These sets of reflections are mostly parallel, with geological consistency in their orientation and a significant extension, reaching from near the top of the buried hill to its deeper parts. Therefore, it is concluded that the steep reflections inside the buried hill are genuine seismic responses caused by real geological conditions. Based on literature research of other offshore buried hill oil fields in China [11–16], seismic data confirm the presence of steep reflections within the buried hill. The steep reflection signals in the study area are real and reliable, closely related to the base faulting. Due to the overall weak reflection energy within the buried hill, directly performing 3D interpretation of the steep faults from the original data is challenging. Therefore, an enhanced processing approach combining steep-angle reflection amplification with low-pass filtering is applied to the original data, aiming to strengthen the steep reflection signals inside the buried hill. The processed seismic data highlight the fracture reflection information (steep reflection signals) within the buried hill, facilitating the depiction of internal base faults.

3.3. Thin-Section Observation

Thin-section samples were collected from eight cored wells and observed under plane-polarized light. A total of 25 samples from drilling cores of the buried hill reservoir were doubly polished, followed by blue epoxy-impregnation and staining with Alizarin red for identification of reservoir lithology (Table 1).

Table 1. Representative lithological description of core samples collected from buried hills in the Beibuwan Basin.

Well No.	Strata	Sample Depth	Thin-Section Image	Lithological Description
Well A	Huanglong Formation	1830 m	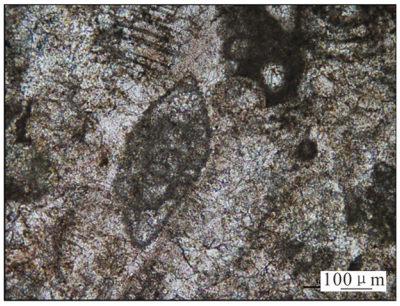	In the mircite of Huanglong Formation, fragments of Fuzulinid organisms were observed. The calcite in the micrite was replaced by dolomite crystals
Well A	C Member	1935 m	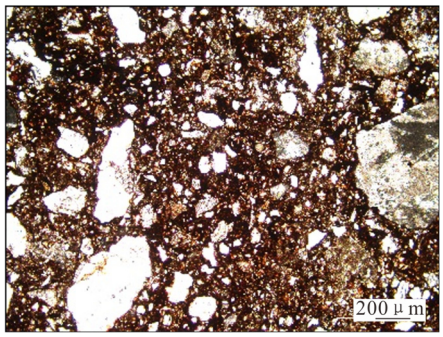	In the sandstone of C Member, the quartz grains exhibit poor roundness and sorting
Well L	S Member	3037 m	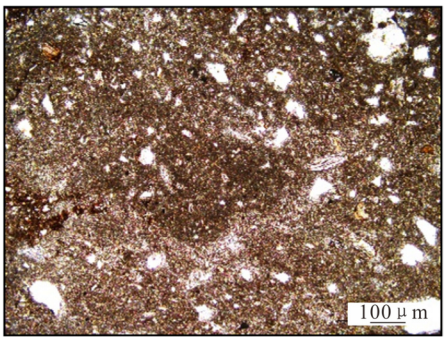	In the mirite of S Member, a few quartz grains with poor roundness and sorting were observed
Well L1	S Member	3062 m	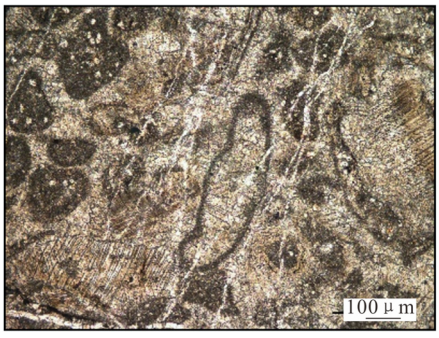	In the mirite of S Member, a fracture cemented by calcite were observed

Table 1. *Cont.*

Well No.	Strata	Sample Depth	Thin-Section Image	Lithological Description
Well D1	Granite basement rock	1483 m	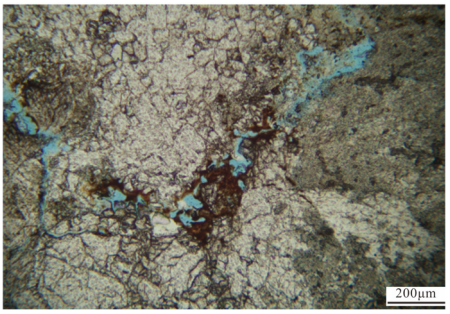	The altered, slightly fractured fine-grained granite shows intense weathering of feldspar, with clay mineralization on the surface and pyrite filling the fractures

4. Results

4.1. Interior Strata of Buried Hills

Strong continuous reflections in seismic profiles are often interpreted as carbonate strata within basement highs [23,24]. However, recent drilling data indicate the presence of large-scale granite intrusions within the basement (Figure 3). Recent findings in the Bohai Bay Basin suggest that granite intrusions appear as chaotic reflections in seismic profiles, while metamorphic basement highs show clear, layered, continuous strong reflections [25]. Granites correspond to chaotic reflections, while metamorphic rocks, especially gneisses, exhibit continuous strong reflection characteristics, similar to those of carbonate rocks [26]. Therefore, this study combines recent drilling data and literature to interpret the internal strata of the basement highs. The seismic profile in the NEE direction, located between the main fault zones 1 and 2, was selected to interpret the internal strata. The basement, composed of Carboniferous limestone, is in contact with the underlying granite basement, forming a superposed basement structure. Clearly, the Carboniferous limestone represents deformed strata, corresponding to the lower Carboniferous M and S Member, which are thick in some areas. The M Member thins out gradually towards the west and may even taper off. The S Member also thins out, and its upper boundary is covered by deformed strata of the C and Z Member. The Carboniferous strata in the current structural depression have been completely eroded (Figure 3). As a result, the Carboniferous deformed strata form the main body of the limestone basement, which is in angular unconformity with the overlying Cenozoic strata. The distribution of the Carboniferous strata is controlled by tectonic evolution, primarily driven by fault activity.

4.2. Negative Structural Inversion and Its Control of the Interior Strata

A negative inversion fault, formed under early compressional stress, undergoes later extension due to the influence of a tensile stress field. This fault has experienced a transition from strong compression to weak compression, followed by extension [27–29]. Based on the formation environment and development characteristics, strata involved in negative inversion can be classified into three types: compressed and eroded sequences, compression–extension transitional subsidence sequences, and extensional faulting sequences [27]. The compressed and eroded sequences, developed under compressional stress, take the form of a wedge that thins toward the reverse fault. The erosion thickness is greatest in the direction of the fault, and internal reflections are often parallel or subparallel [30]. The compression–extension transitional sequences overlie the fault direction and have a similar external form to the compressed and eroded sequences, showing a wedge that thins towards the reverse fault. The extensional faulting sequences exhibit an external wedge shape that thins away

from the fault. The overlying direction extends from the near-fault end to the far-fault end, indicating that the extensional faults control the sedimentary filling process of the extensional faulting sequences (Figure 4).

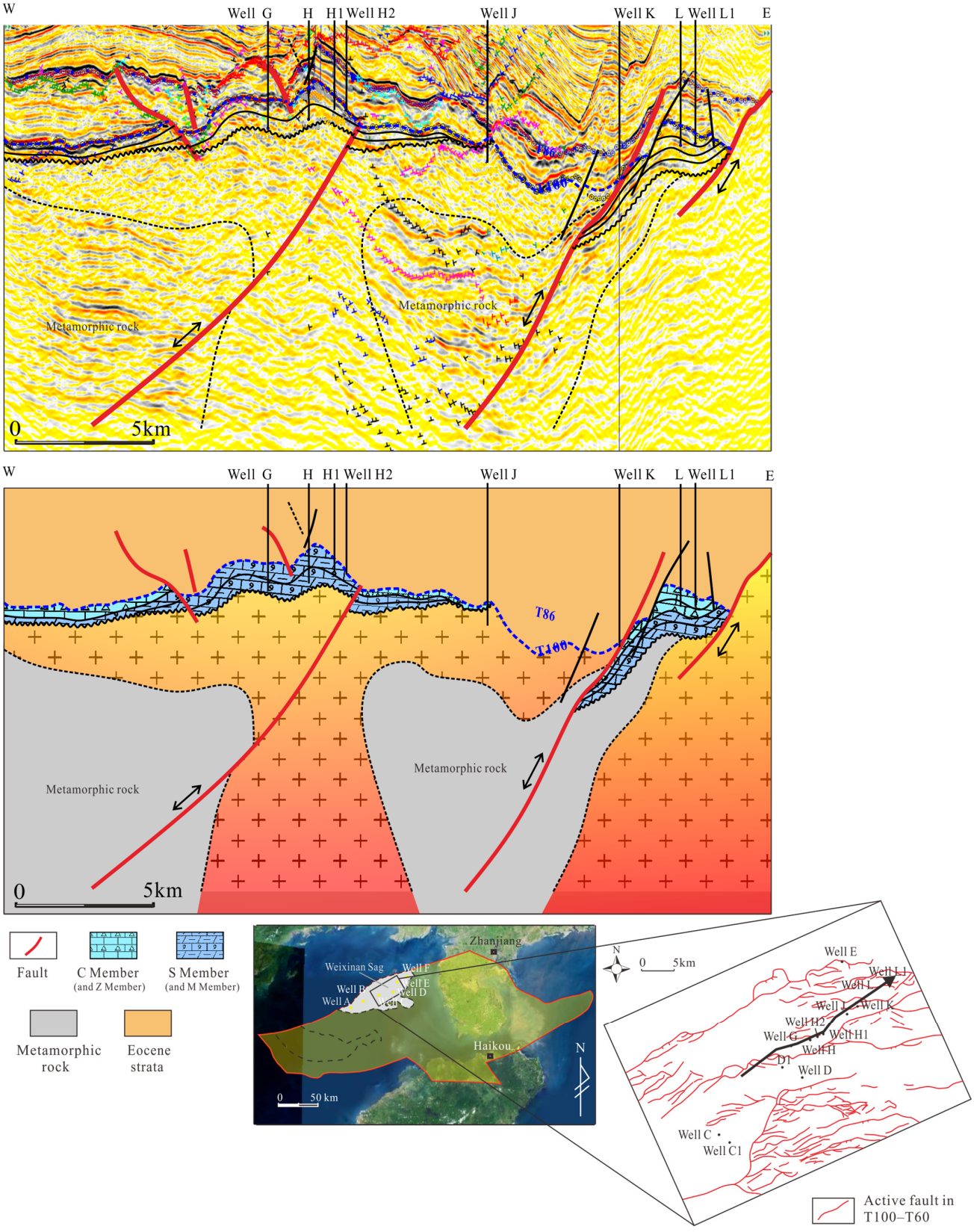

Figure 3. Interior stratigraphic section of buried hills and column chart of Carboniferous strata in NW Beibuwan Basin.

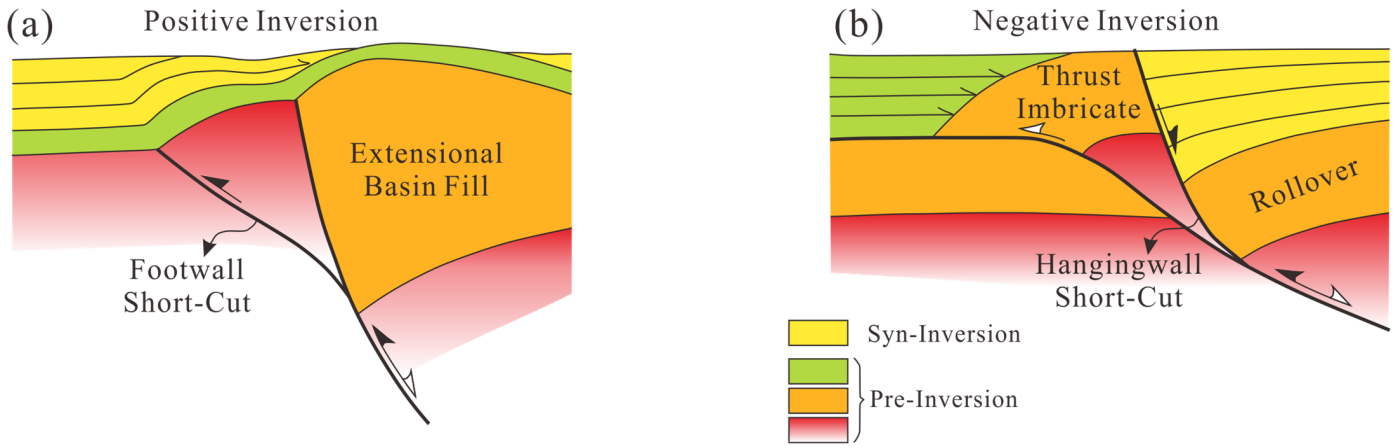

Figure 4. Cartoon summary of the contrasting simplified geometries of structures with (**a**) positive inversion versus (**b**) negative inversion (modified from [27]).

Reverse anticlines and reverse faults are significantly different. Reverse faults result from later reverse motion on pre-existing faults, meaning their formation requires the presence of an earlier fault system. The early faulting is a prerequisite for the development of reverse structures. The formation of reverse anticlines is generally unrelated to faulting. They are usually the result of late-stage uplift of an early sedimentary center under compressional stress. In vertical profiles, they typically exhibit the characteristic "downward concave, upward convex" shape [31,32].

In addition to the long-term reverse faults of Weixinan Master Fault (Fw), No. 1 Master Fault (F1), No. 2 Master Fault (F2), and No. 3 Master Fault (F3), there are also secondary faults branching from the Master Fault and smaller, short-lived reverse faults (i.e., pre-existing internal faults) [33,34]. Recognizing these smaller reverse faults is significant, as they control the local stratigraphic development. For example, F1 and F2 show clear reverse fault signatures in seismic profiles (Figure 5). The Changliu Formation between T90 and T100 thins noticeably near the faults, exhibiting a thin-skinned structural style. Before the fault experiences extension, the fault throw is small, and seismic interfaces display a clear upward curvature (indicating reverse normal traction). The fault only begins to transition into a normal fault once it intersects the Cenozoic strata. Additionally, these faults typically have a shallow dip at depth and often exhibit detachment features, providing key evidence of early compressional shear deformation. The upper dip angle of these faults increases, reflecting the superposition of early reverse thrust and later extensional properties (Figure 5). Similar reverse fault signatures can be observed in seismic profiles. Two short-lived reverse faults (Fx_1 and Fx_2) display reverse motion before extension and jointly control the limited distribution of the Carboniferous strata, particularly the C and Z Members of the Lower Carboniferous (Figure 5).

Before determining the distribution of the Carboniferous strata in the buried hills, it is essential to analyze the control exerted by the negative inversion fault on the strata distribution. The pre-inversion fault is a reverse fault, with the Carboniferous strata on the hanging wall located at higher elevations, experiencing intense diagenesis and leaching. In contrast, the Carboniferous strata on the footwall, near the fault, are at lower elevations and undergo weaker diagenesis. As a result, the Carboniferous strata on the hanging wall and footwall of the negative inversion fault typically belong to different geological periods. The differing distribution of strata indicates that two periods of stress-induced fault inversion have governed the varying erosion and distribution of the Carboniferous strata. The complexity of the Carboniferous strata distribution can be attributed to two separate periods of negative inversion faulting. One is a short-term negative inversion fault with

a NE–SW orientation, while the other is a long-term, active negative inversion fault with a NEE–SWW strike. The strikes of these two fault periods intersect at a sharp angle. The strata at the top of buried hill indicate that the hanging wall of the long-term negative inversion fault consists of granite, while the footwall contains the lower Carboniferous. The reverse thrust activity of the fault has entirely eroded the Carboniferous strata on the hanging wall, while only partial erosion has affected the strata on the footwall (Figure 6). The hanging wall of the short-term negative inversion fault contains the M Member and S Member, while the footwall holds the C Member (or Z Member) [24], indicating that the reverse thrust activity has severely eroded the Carboniferous strata on the hanging wall, with comparatively less erosion on the footwall.

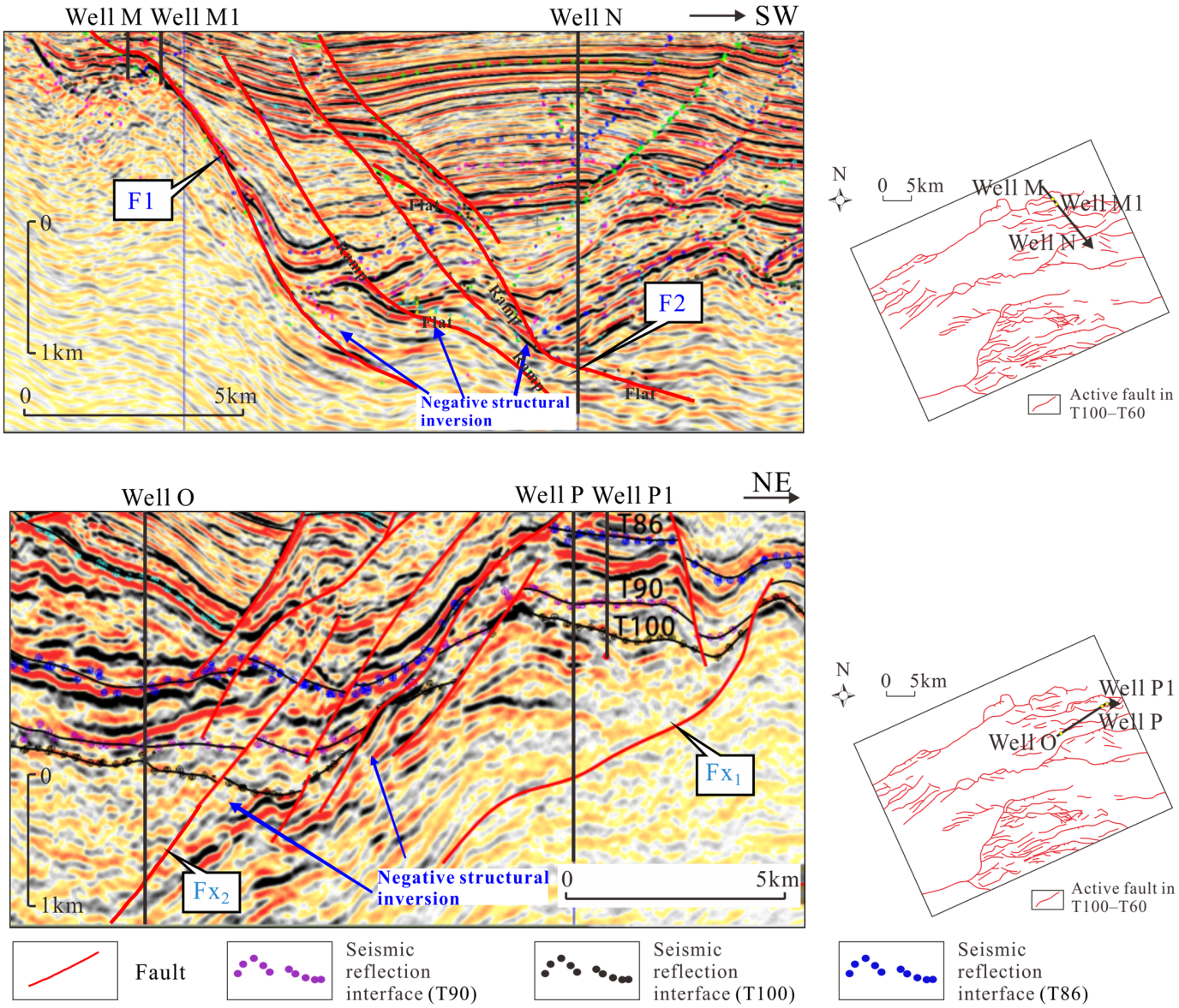

Figure 5. Seismic profiles of negative structural inversion. F1 and F2 are long-term active reverse faults; Fx_1 and Fx_2 are short-term active reverse faults.

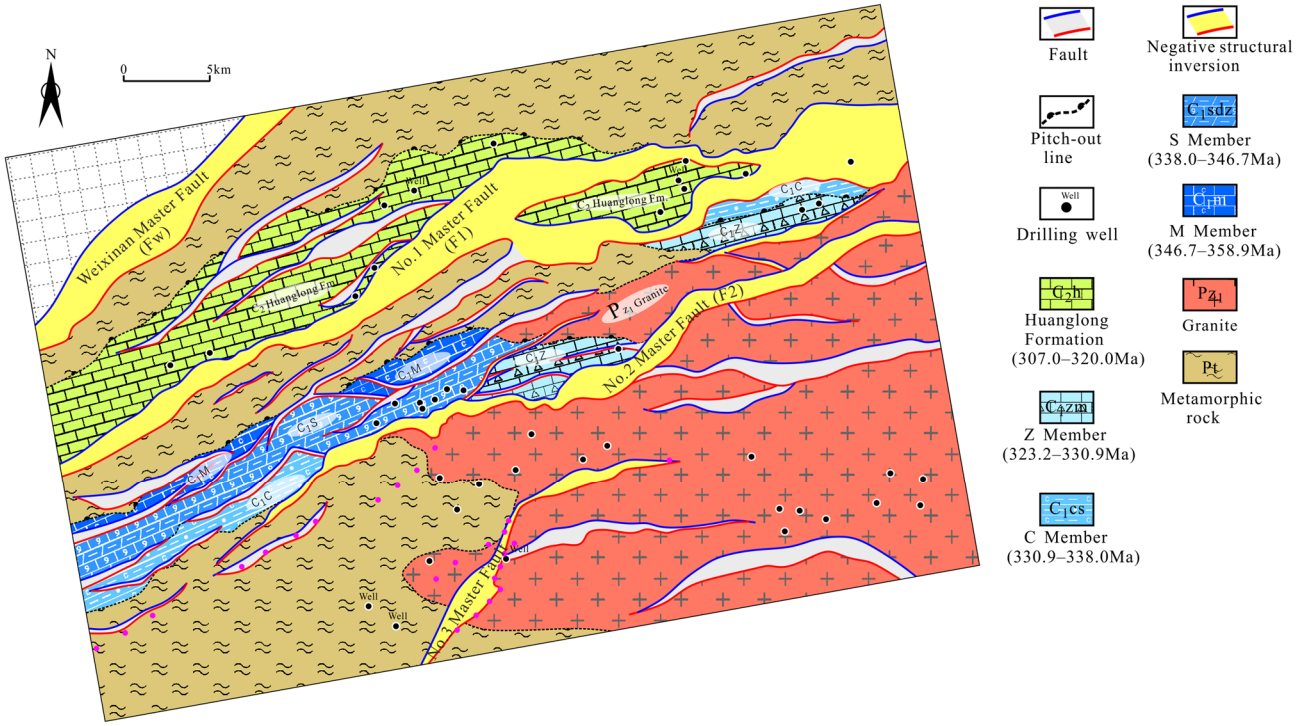

Figure 6. Distribution of strata at the top of buried hill in the Weixinan Sag, Beibuwan Basin.

Early granite intrusions caused localized uplift, which established the paleogeography prior to Carboniferous sedimentation. The topographic variations in the sedimentary paleogeography led to a gradual thinning of the Carboniferous strata toward the east. During the Late Hercynian, Indosinian, and Yanshanian orogenies, two phases of compressive stress in different directions generated two sets of reverse faults with different strikes, controlling the degree of erosion of the Carboniferous strata. Within the study area, the geological age of the strata at the top of these buried hills gradually becomes younger from the SE to the NW direction (Figure 6). In the direction near the footwall of the negative inversion fault, the geological age of the strata becomes progressively younger, and the Carboniferous strata generally dip to the SE [34].

4.3. Stress Field and Tectonic Fault Activity

4.3.1. Late Ordovician-Silurian Period

The study area belongs to Yunkai Massif during the Early Paleozoic (Figure 7). The Early Paleozoic was a stage of rift development, with the Yunkai Massif being part of the South China platform during this period [20,21]. Crustal movements were primarily vertical, with no significant development of faults or folds (Figure 7). A sequence of shallow marine-like limestone facies was deposited within the Beibuwan Basin during this time [35,36]. The Early Paleozoic era in the Beibuwan Basin underwent a series of tectonic, magmatic, and metamorphic evolution processes [20,21]. Stage 1: Initial Downthrust Stage (≥460 Ma). Around 460 Ma or earlier, the remnant ocean basin in South China began subducting beneath the southeastern margin of the Yunkai Massif from a northwest to southeast direction [36]. Stage 2: Downthrust Stage (460–440 Ma). During this period, the subducting young and thermally active oceanic plate, along with overlying sediments, underwent dehydration and partial melting at varying depths. The resulting fluids and melts interacted with the overlying mantle wedge, triggering partial melting and leading to the formation of volcanic rocks. Stage 3: Collision and Post-Collision Stage (≤440 Ma). Continental collision caused significant crustal thickening, followed by

post-orogenic extension, collapse, and delamination. These processes led to widespread emplacement of granites, high-temperature granulites [37], and mafic-felsic intrusions in the Beibuwan Basin.

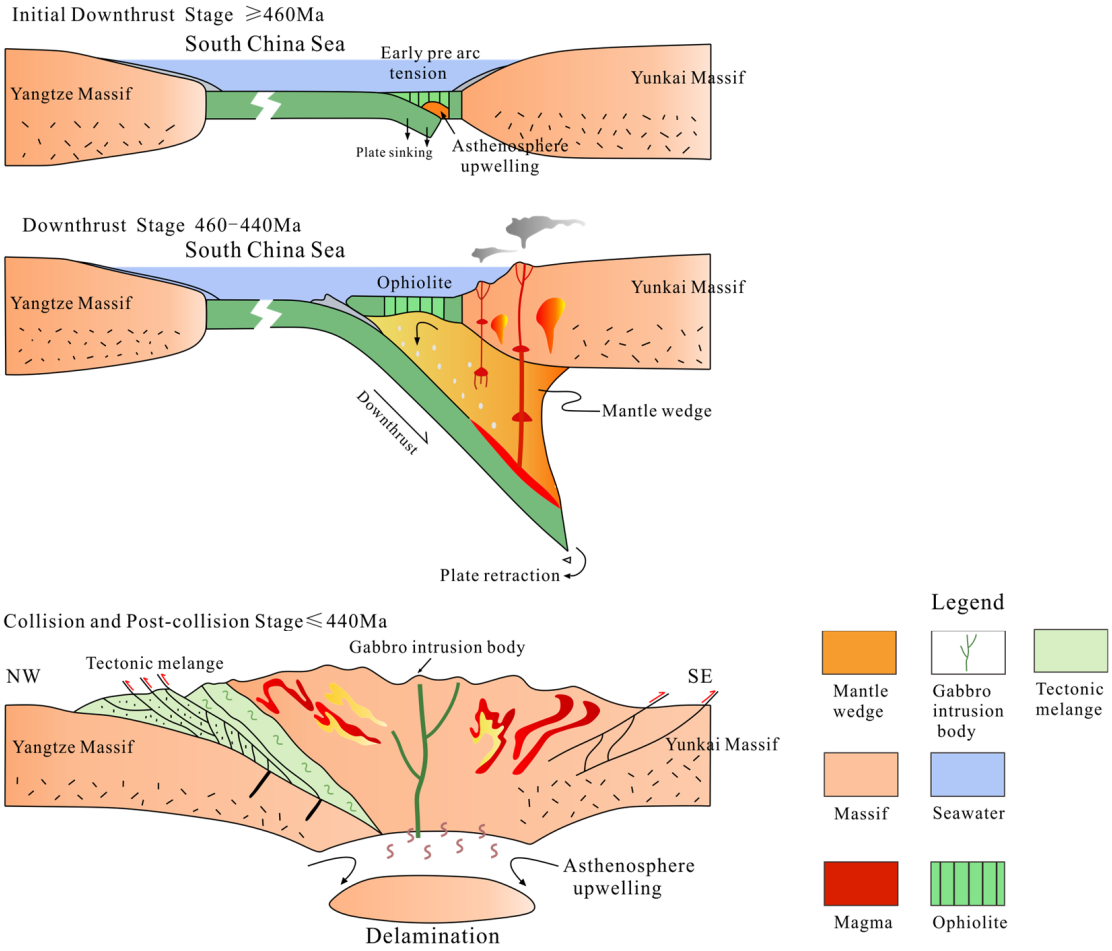

Figure 7. Early Paleozoic (460–400 Ma) tectonic evolution model of Beibuwan Basin (belonging to the Yunkai Massif) (modified from [36]).

At the end of the Silurian, the crust was uplifted due to NW-SE compressional stress during the Caledonian orogeny [22]. The rifting basin underwent folding and inversion, and the Beibuwan Basin entered the stage of platform development [34]. During this period, broad anticlines and synclines developed, and NE-strike regional faults began to form [22]. The Weixinan Master Fault (Fw) began to form and thrust during this time, while magma along the southeastern margin of the Beibuwan Basin intruded the metamorphic basement through underplating or fault-related processes [38]. Granite intrusions caused uplift, resulting in a paleogeography characterized by significant elevation differences. On the south Beibuwan Basin, magma intruded at higher elevations, overlying relatively thin metamorphic rocks, all of which were above the Devonian sea level and subject to differential diagenesis and erosion.

4.3.2. Permian-Triassic Period

In the early Devonian, the Beibuwan Basin retained the paleogeomorphology formed by the Caledonian orogeny, characterized by thrust faulting and imbricate structures [22]. In the northwest and southeast of the Weixinan Sag, the axis of the anticlines began to be eroded [24]. Within the syncline area, clastic sediments began to accumulate [21]. During the Middle Devonian, influenced by the Hercynian movement, the Beibuwan

Basin experienced overall subsidence and entered the foreland basin stage [20]. In the Carboniferous, influenced by the Hercynian orogeny, the Weixinan Master Fault (Fw) experienced retrograde motion. This led to widespread, continuous deposition of coastal clastic rocks and shallow marine carbonates, forming the Lower Carboniferous M, S, C, and Z Members, as well as the Upper Carboniferous Dapu and Huanglong Formations (Figure 8). In some areas, overlying metamorphic rocks were completely eroded, exposing granite that underwent diagenesis by atmospheric freshwater leaching. In the Late Permian, under the influence of NE–SW compressive stress from the Dongwu Movement, buried hill interiors developed fractures, leading to the formation of local thrust structures. The overlying Carboniferous strata were subjected to differential erosion. During the Early Permian, the Paleo-Tethys Ocean subducted beneath the South China Plate [20], and the Weixinan Sag was influenced by NE-directed compressive stress from the Indochina block.

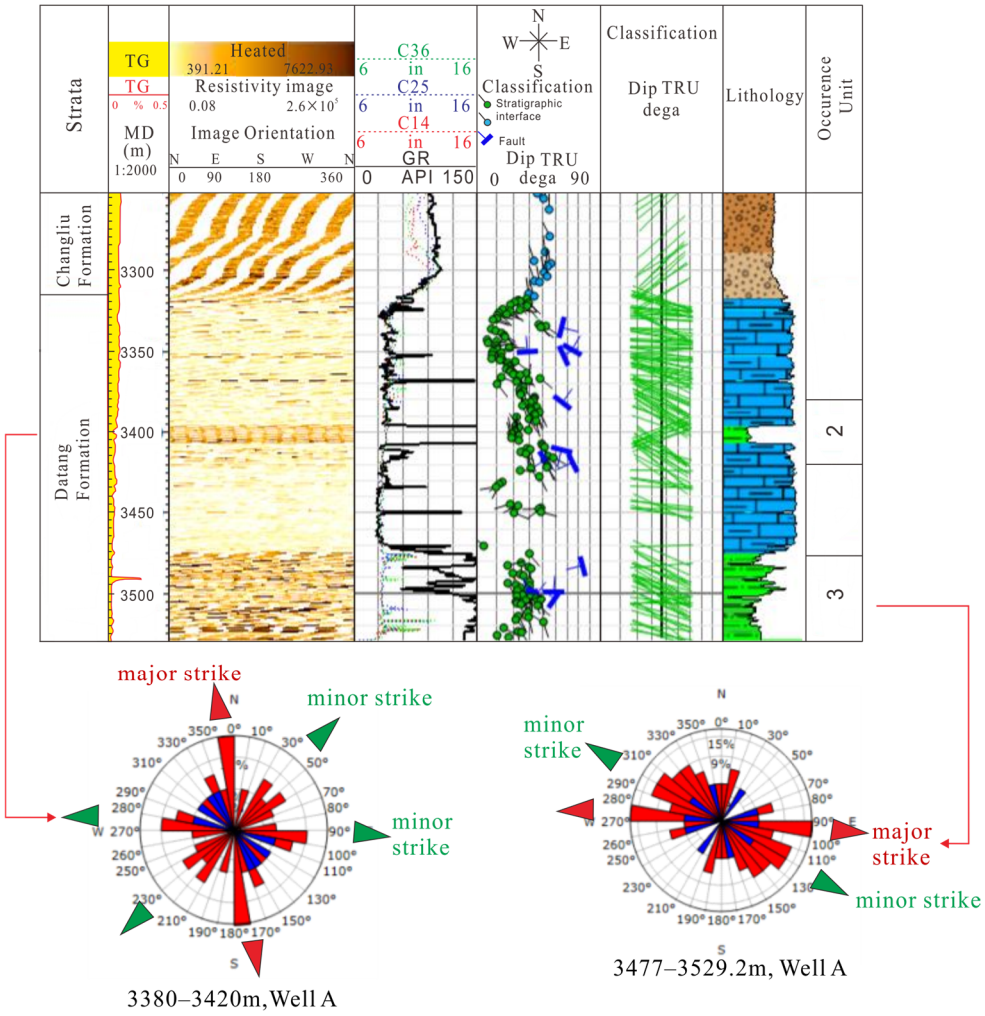

Figure 8. Stratigraphic strike histogram of carbonate buried hill in the Weixinan Sag, Beibuwan Basin (based on logging data).

4.3.3. Triassic-Cretaceous Period

During the Late Permian to Middle Triassic, the SE–NW-directed compressive stress of the Indosinian orogeny reactivated NE-directed Caledonian faults (Figure 9), resulting in a series of NE-directed thrust fault structures [39]. Prominent NE-directed thrust faults, including the Weixinan Master Fault (Fw), No. 1 Master Fault (F1), No. 2 Master Fault (F2), and No. 3 Master Fault (F3), caused differential diagenesis and erosion of the Carboniferous strata. The stress primarily originated from the southeast, pushing the hanging walls of the

Master Faults above sea level, where they were subjected to intense erosion. The footwall of No. 1 Master Fault (F1) was situated at a lower elevation and experienced less erosion. During the Yanshanian Movement, tectonic uplift further exposed and eroded the buried hills [22–24]. Prior to the deposition of Cenozoic strata, the buried hills underwent continued diagenesis, leaching, and erosion. Following this, due to subsidence, the remaining Carboniferous strata in the Weixinan Sag were once again buried.

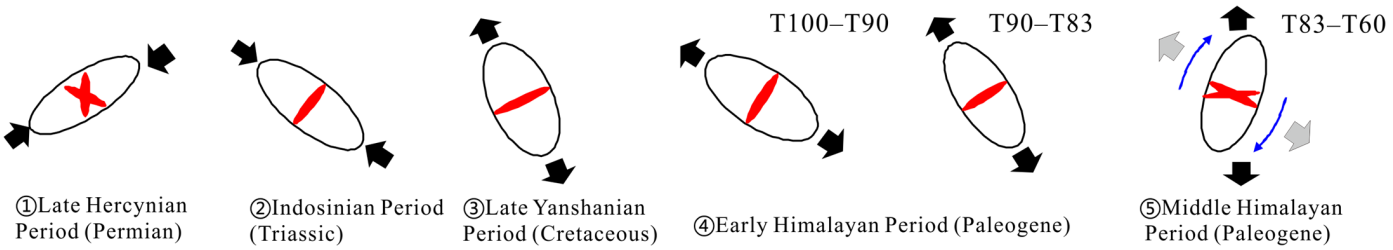

Figure 9. Schematic diagram of stress field evolution process in the Weixinan Sag, Beibuwan Basin.

4.3.4. Paleogene Period

In the early stages of the Himalayan orogeny [22], regional northwest–southeast extension triggered a progressive retrograde motion along the Weixinan Master Fault (Fw) and the No. 1, No. 2, and No. 3 Master Faults. The retrograde motion along No. 3 Master Fault (F3) occurred last, interrupting the deposition of Cenozoic strata. Tectonic activity was most intense in the southwest of the study area and gradually weakened toward the northeast [34]. During the Indosinian orogeny, the buried hills developed extensional fractures due to regional stretching. In the late stages of the Himalayan orogeny, extensional and shear movements ceased, and the positions of the Paleozoic buried hills were firmly established [40].

5. Discussion

5.1. Controlling Effect of Faults on Buried Hill Reservoirs

Petrographic analysis shows that the reservoir space of buried hills in the Beibuwan Basin consists of structural fractures (Figure 10a,b), dissolved fractures (Figure 10c,d), and dissolved pores (Figure 10e). This indicates that the formation of buried hill reservoirs is controlled by both diagenesis processes and tectonic modifications (Figure 10f). The tectonic evolution of the area suggests that the formation of buried hills occurred in two distinct phases. The first phase involved the Late Ordovician-Silurian period granitic intrusions, which caused a basement uplift, forming the basement-involved buried hills. The second phase occurred during the Hercynian orogeny, when reverse thrusting uplifted the Carboniferous limestone strata and the underlying basement rocks, creating new phase buried hills. The development of faults and fractures is well-correlated. Specifically, the larger the fault displacement and the closer to the fault, the denser the fractures become. Faults are considered key to the vertical extension of the weathered cap reservoir into the internal reservoir of the buried hills. However, only the tectonic fractures formed prior to the development of the buried hills play a dominant role in controlling the scale and distribution of diagenesis-induced reservoirs. Consequently, the faults and fractures formed during the Caledonian orogeny facilitated the atmospheric freshwater diagenesis of the buried hills in the second phase. However, Permian-Triassic fault activity does not align with the timing of buried hill reservoir formation. Previous studies suggest that faults and fractures formed earlier are more likely to be fully cemented by calcite, thereby reducing their potential as effective reservoir spaces. The Late Paleocene to Oligocene period marks the final stage of the extensional rifting in the Beibuwan Basin. This suggests that tectonics,

rather than global climate changes from the Paleocene to Oligocene [41,42], explains the sedimentation–erosion processes during this time. During this period, faults formed were most susceptible to later hydrocarbon and organic acid charging, which interrupted calcite cementation and preserved reservoir space.

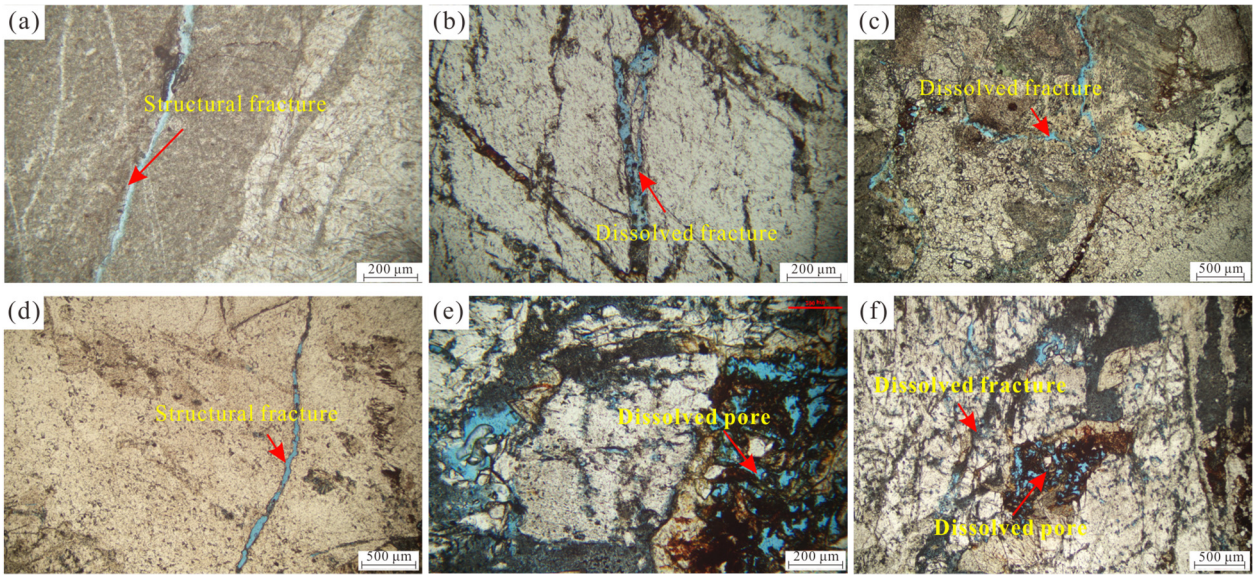

Figure 10. Microscopic characteristics of reservoir spaces in buried hill reservoirs in Beibuwan Basin. (**a**) Structural fractures, Well A, 3062 m. Plane-polarized light. (**b**) Dissolved fractures, Well B, 1486 m. Plane-polarized light. (**c**) Dissolved fractures, Well B, 1547 m. Plane-polarized light. (**d**) Structural fractures, Well C, 1484 m. Plane-polarized light. (**e**) Dissolved fractures, Well C, 1481 m. Plane-polarized light. (**f**) Dissolved fractures and pores, Well C, 1481 m. Plane-polarized light.

5.2. Controlling Effect of Faults on Hydrocarbon Accumulation

Well logging and drilling data from the Liushagang Formation indicate that it is divided into three members: the third, second, and first members, from bottom to top (Figure 11). The first and third members are primarily composed of mudstone. The lower part of the second member contains a set of black shale, while the middle and upper parts consist mainly of dark mudstone. Extensive drilling results show that the source rock in the second member has a stable thickness and a wide distribution. Notably, the black shale at the base of the second member is a sedimentary product of a semi-deep to deep lake environment under a lacustrine transgression system [43,44]. Core sample TOC data indicate that the black shale in the second member has a TOC value greater than 2 wt.% [40], classifying it as source rock [45–49]. The crude oil from the buried hill reservoir was compared with the Liushagang second member source rocks for biomarker compounds (including m/z 191 and m/z 217) [40,50–52]. Biomarker compound analysis further confirms that the hydrocarbons in the buried hill reservoirs mainly originate from the second member of the Liushagang Formation [53–59]. The formation of the second member corresponds to the early to mid-Eocene period. During this period, regional extensional stress rotated clockwise to an NNW–SSE direction. This led to strong NE-directed fault activity, with basin tectonics evolving from simple faulting to compression, folding, fault translation, and strike-slip. Extensional rifting controlled the deepening and expansion of the basin center, promoting large-scale organic matter accumulation and preservation, which in turn favored the formation of thick, high-quality source rocks [40]. In the basin center, the source rock in the second interval can reach a maximum thickness of 140 m, with wide distribution and good continuity. In contrast, the source rocks in the first and third members have more limited distribution (Figure 11), and the first interval has lower maturity. Therefore,

the influence of faults on hydrocarbon accumulation is primarily associated with their control over the hydrocarbon generation and expulsion phase in the second member of the Liushagang Formation (Figure 12a,b). The current burial depth of the source rock in the second interval ranges from 2100 m to 2500 m, with a maturity of 1.0–1.5%, placing it within the oil generation window for significant hydrocarbon formation [57–59]. After the Miocene, extensional rifting in the Beibuwan Basin ceased, tectonic activity weakened, and the basin entered a subsidence phase. Consequently, later extensional faults are more favorable for the migration of hydrocarbons from the source rocks into the buried hill reservoirs, facilitating their accumulation. The Late Eocene to Oligocene period marks the final phase of extensional fault activity in the Beibuwan Basin. During this time, the faulting was most closely timed with hydrocarbon expulsion (Figure 13), maximizing the effectiveness of fault communication between the source rocks and reservoirs (Figure 14).

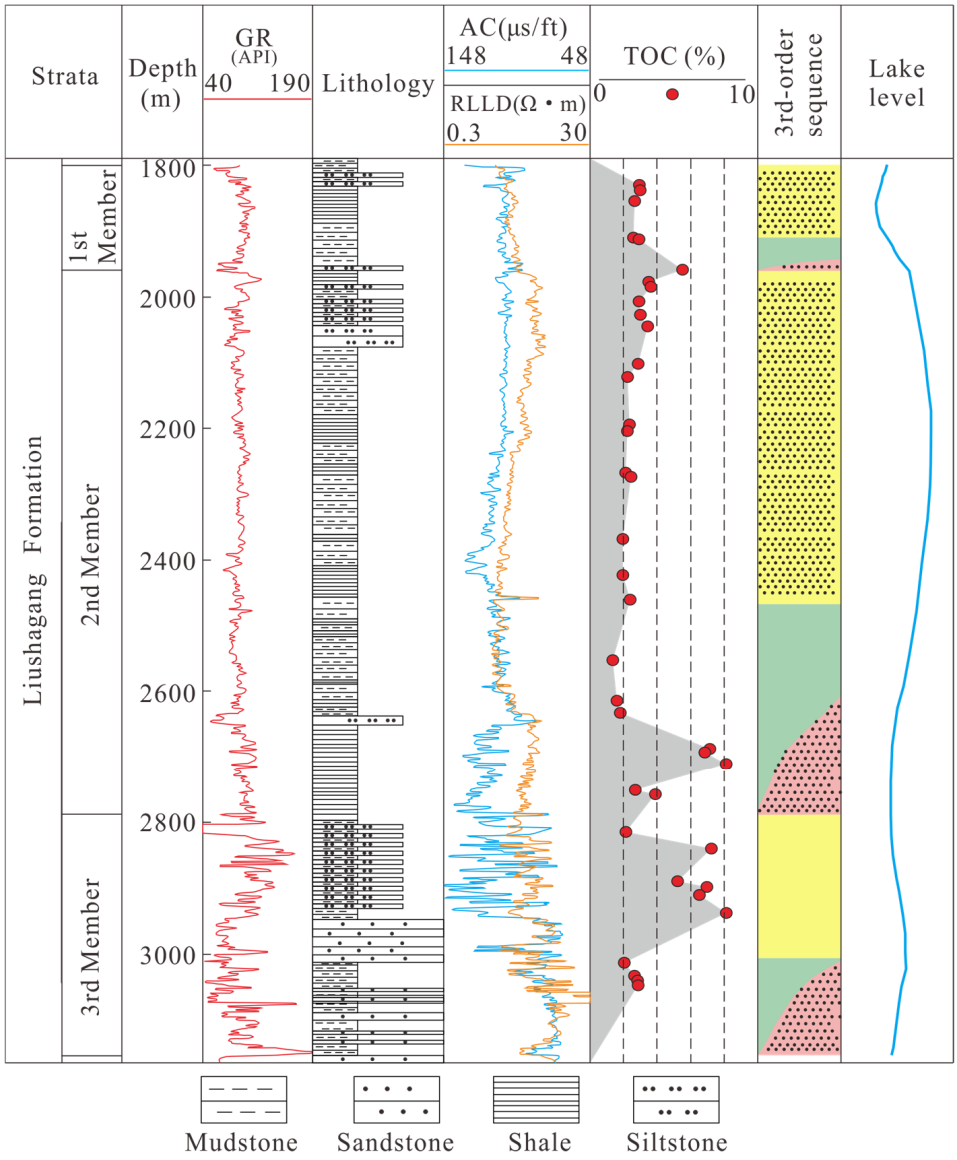

Figure 11. Comprehensive column chart of hydrocarbon source rock strata (Liushagang Formation) (modified from [40,59]).

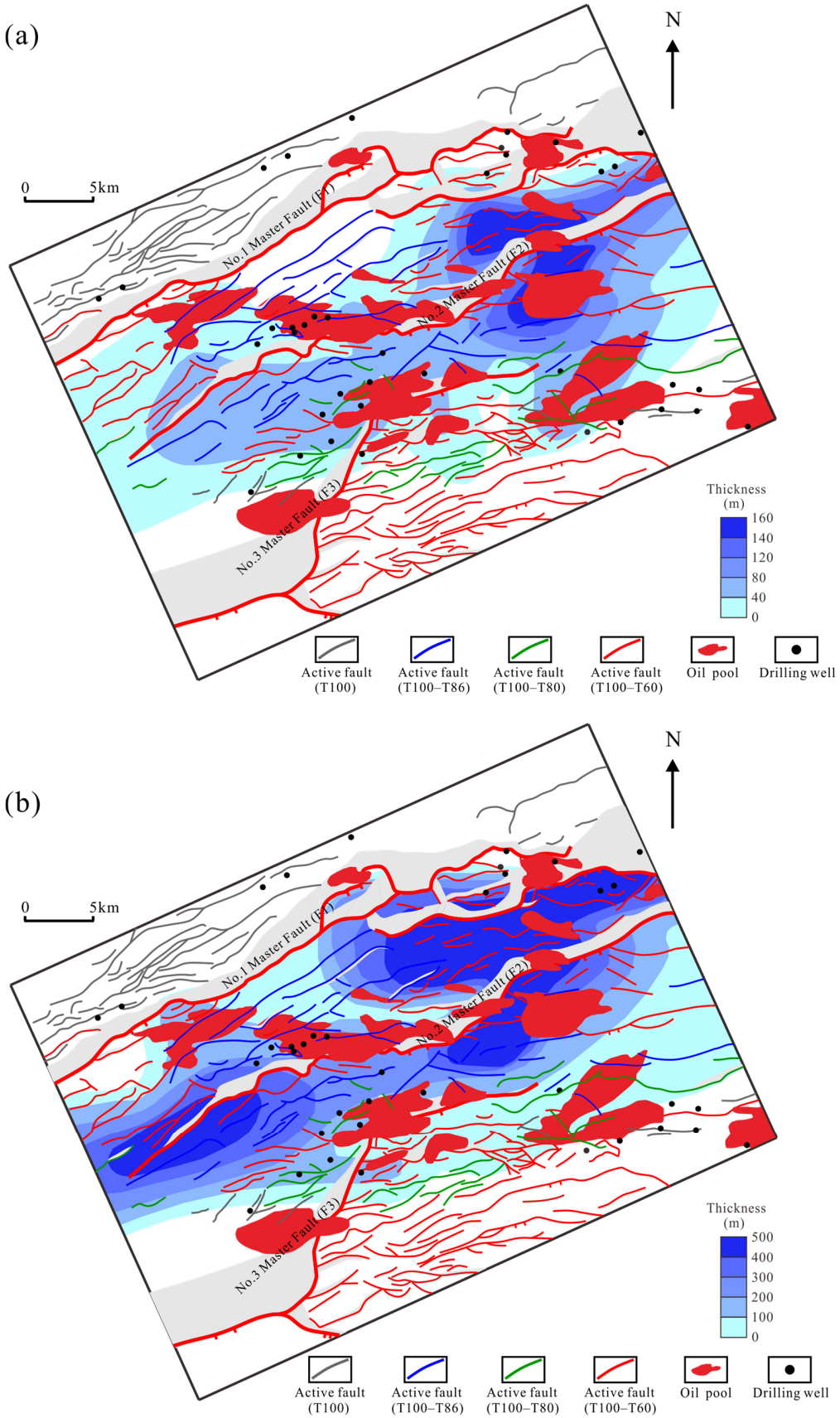

Figure 12. (**a**) Superimposition of organic-rich shale thickness, fault of different periods, and oil pool in the Liushagang Formation second member. (**b**) Superimposition of dark mudstone thickness, fault of different periods and oil pool in the Liushagang Formation second member. The 3D seismic area is shown in Figure 1a.

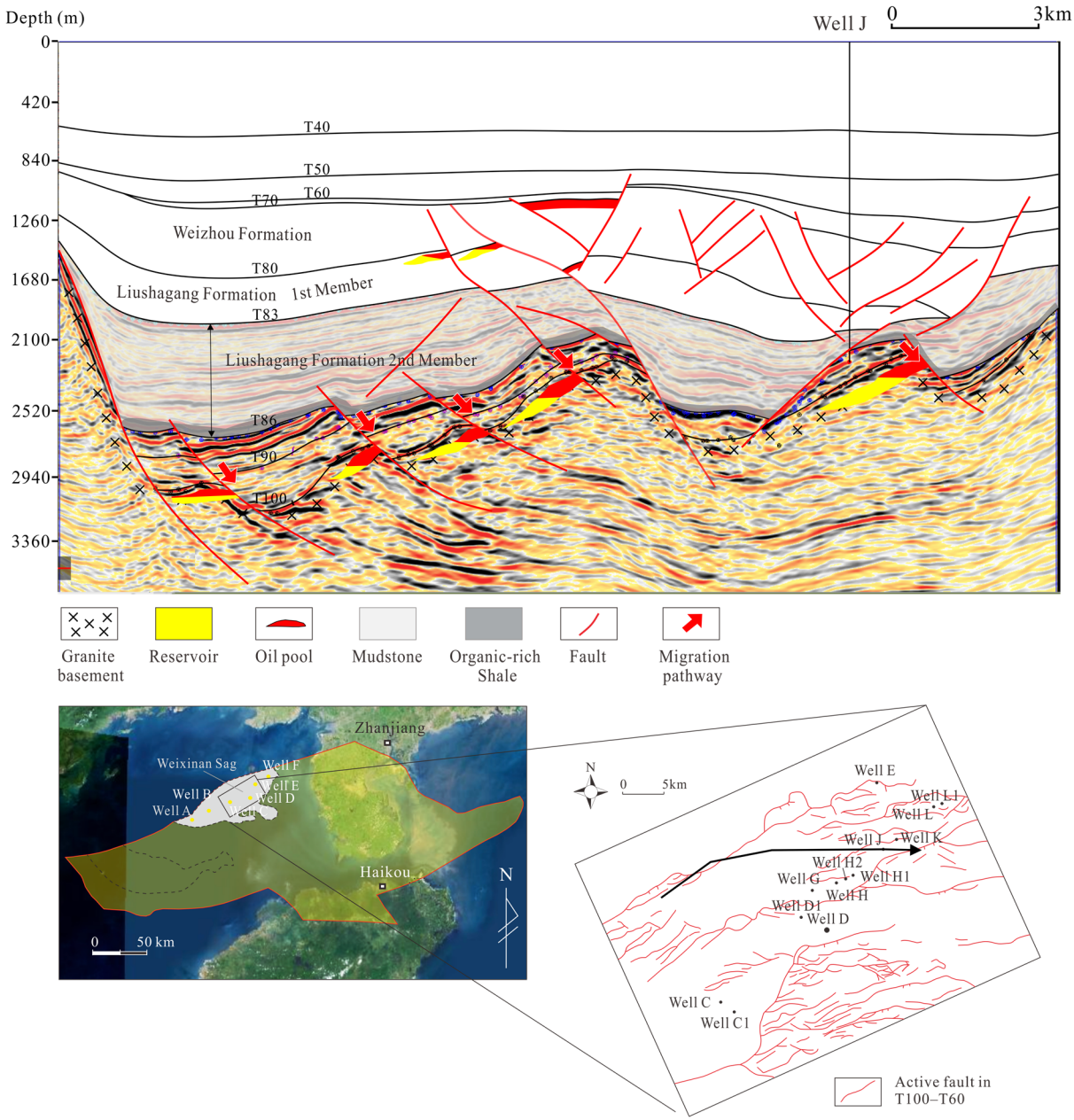

Figure 13. Cross-section of hydrocarbon accumulation in buried hill reservoirs of Beibuwan Basin.

The mudstone and shale in the Beibuwan Basin serve both as source rocks and as seal rocks. During the Paleogene, the Beibuwan Basin experienced three periods of lake basin expansion. As a result, thick layers of semi-deep lake mudstone and shallow lake mudstone were deposited within the Liushagang and Weizhou formations, making them excellent regional seal rocks [60]. During the Neogene, multiple sea-level changes led to the deposition of several sets of shallow marine mudstone sequences. The first member of the Jiaowei Formation developed thick regional marine mudstones. Drilling confirmed that the mudstones and dense layers within the buried hills, the tight layers of the Changliu Formation, the shales and lacustrine mudstones of the Liushagang and Weizhou formations [22], as well as the marine mudstones from the Neogene, all exhibit excellent sealing properties (Figure 14).

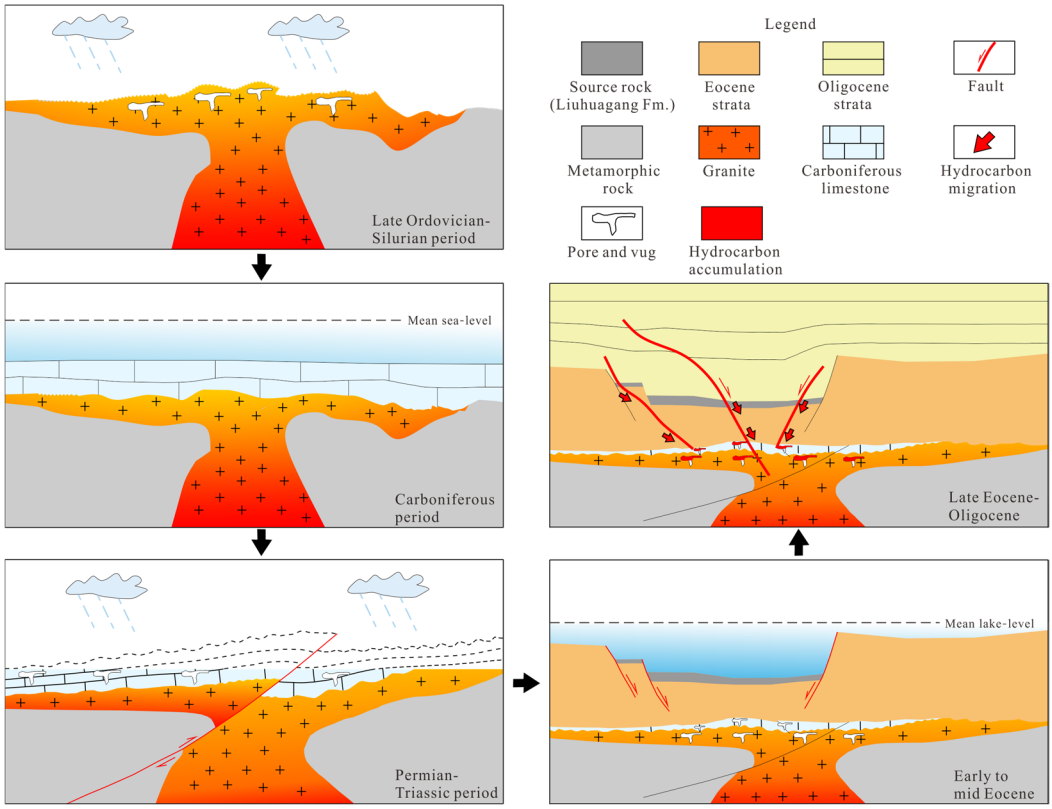

Figure 14. Conceptual model showing complex fault system contribution to the hydrocarbon accumulation in buried hill reservoirs of Beibuwan Basin.

6. Conclusions

(1) The buried hills in Beibuwan Basin are formed in two different tectonic stages. The first stage belongs to the magma diapirism activity of the Late Ordovician-Silurian period, and the second stage belongs to the reverse thrust activity of the Permian-Triassic period. The fault systems formed by two periods of tectonic activity were, respectively, altered into basement buried hills and limestone buried hills.

(2) The negative structural inversion controls the distribution and interior stratigraphic framework of the deformed Carboniferous strata in the limestone buried hill. Under multiple phases of stress evolution, negative inversion structures primarily influence reservoir development in three ways: ① They drive the development of fracture networks, providing initial pathways for subsequent reservoir modification; ② They control differential erosion of strata, exposing favorable lithologies that form the material basis for high-quality reservoirs; ③ They shape paleogeographic highs, creating favorable conditions for epigenetic karst processes. Fault activity induces the migration of deep fluids, enhancing the intensity of burial dissolution processes.

(3) The reservoir space of the buried hill reservoir is composed of dissolved pores, fractures, and structural fractures. The faults and derived fractures of the Late Ordovician-Silurian period and Permian-Triassic period, respectively, promoted the diagenesis and erosion of these buried hills by atmospheric freshwater, while also forming reservoir spaces, although the impact of fault activity after the Hercynian period on the formation of buried hill reservoirs is small. However, the faults formed during the late Eocene-Oligocene are not conducive to calcite cementation, thus facilitating the preservation of the reservoir space formed earlier.

(4) The control of hydrocarbon accumulation in buried hill reservoirs by fault activity is reflected in two aspects: on the one hand, the early to mid-Eocene extensional faulting activity directly controlled the depositional process of lacustrine source rocks; on the other hand, the Late Eocene-Oligocene, which is closest to the hydrocarbon expulsion period, is the most effective fault activity period for connecting Eocene source rocks and buried hill reservoirs.

Author Contributions: Conceptualization, A.L. and F.X.; methodology, G.X.; validation, C.F.; formal analysis, M.L.; investigation, F.J. and X.X.; data curation, X.Z.; writing—original draft preparation, A.L. and F.X.; writing—review and editing, G.X. and B.X.; visualization, M.L.; supervision, F.J. and X.X.; project administration, X.Z. and B.X. All authors have read and agreed to the published version of the manuscript.

Funding: This research was funded by the National Natural Science Foundation of China, grant number 42302186.

Data Availability Statement: The original contributions presented in this study are included in the article. Further inquiries can be directed to the corresponding author.

Conflicts of Interest: Authors Caiwei Fan, Ming Li, and Fan Jiang are employed by the China National Offshore Oil Corporation. The remaining authors declare that the research was conducted in the absence of any commercial or financial relationships that could be construed as a potential conflict of interest.

References

1. Landes, K.K.; Amoruso, J.J.; Charlesworth, L.J., Jr.; Heany, F.; Lesperance, P.J. Petroleum resources in basement rocks. *AAPG Bull.* **1960**, *44*, 1682–1691. [CrossRef]
2. Magoon, L.B.; Dow, W.G. The petroleum system. In *The Petroleum System—From Source to Trap: American Association of Petroleum GeologistsMemoir 60*; Magoon, L.B., Dow, W.G., Eds.; American Association of Petroleum Geologists: Tulsa, OK, USA, 1994; pp. 3–24.
3. Christensen, R.J.; Hendricks, M.L.; Eisel, J.D. *Mississippian Buried Hills Reservoirs Along the Northeastern Flank of the Williston Basin, Canada and United States*; Wiley-Blackwell: Hoboken, NJ, USA, 2012.
4. Cuong, T.X.; Warren, J.K. Bach ho field, a fractured granitic basement reservoir, Cuu Long Basin, offshore se Vietnam: A "buried-hill" play. *J. Pet. Geol.* **2009**, *32*, 129–156. [CrossRef]
5. Han, C.; Tian, J.; Hu, C.; Liu, H.; Wang, W.; Huan, Z.; Feng, S. Lithofacies characteristics and their controlling effects on reservoirs in buried hills of metamorphic rocks: A case study of late Paleozoic units in the Aryskum depression, South Turgay Basin, Kazakhstan. *J. Pet. Sci. Eng.* **2020**, *191*, 107137. [CrossRef]
6. Tong, X.; Zuan, H. Buried-hill discoveries of the Damintun Depression in North China. *AAPG Bull.* **1991**, *75*, 780–794. [CrossRef]
7. Wang, Z.; Jiang, Q.; Wang, J.; Long, G.; Cheng, H.; Shi, J. Hydrocarbon accumulation characteristics in basement reservoirs and exploration targets of deep basement reservoirs in onshore China. *Pet. Explor. Dev.* **2024**, *51*, 28–38. [CrossRef]
8. Robert, F. Oil Production from Fractured Pre-Cambrian Basement Rocks in Central Kansas. *Bull. Am. Assoc. Pet. Geologists* **1953**, *37*, 300–313.
9. Chung-Hsiang, P. Petroleum in Basement Rocks. *AAPG Bull.* **1982**, *66*, 1579–1643. [CrossRef]
10. Smith, E. Basement Reservoir of La Paz-Mara Oil Fields, Western Venezuela: GEOLOGICAL NOTES. *Maracaibo Venez.* **1956**, *40*, 380–385.
11. Xu, C.; Wang, Q.; Zhu, H.; Liu, X.; Feng, C.; Hu, B. Hydrothermal alteration mechanisms of an Archaean metamorphic buried hill and the models for reservoir zonation, Bozhong depression, Bohai Bay Basin, China. *Mar. Pet. Geology* **2024**, *164*, 106843. [CrossRef]
12. Kosachev, I.P.; Kayukova, G.P.; Mikhailova, A.N. Features of composition of oil extracts from the rocks of basement and sedimentary stratums of the Novo-Elkhovskoye field of Tatarstan. *Pet. Sci. Technol.* **2019**, *37*, 1016–1024. [CrossRef]
13. Gao, X.; Pang, X.; Li, G.; Chen, Z.; Shan, J.; Liu, F. Complex petroleum accumulating process and accumulation series in the buried-hill trend in the rift basin: An example of Xinglongtai structure trend, Liaohe subbasin. *Sci. China Ser. D Earth Sci.* **2008**, *51*, 108–116. [CrossRef]
14. Wang, Y.; Zhan, X.; Zhou, X.; Gao, Y.; Wang, S.; Xia, J. The geochemical study of oil-oil and oil-source rock correlations in the Wushi Sag of the Beibu Gulf Basin, South China Sea. *Front. Earth Sci.* **2024**, *10*, 850922. [CrossRef]

15. Yi, J.; Li, H.; Shan, X.; Hao, G.; Yang, H.; Wang, Q. Division and identification of vertical reservoir units in Archaeozoic metamorphic buried hill of Bozhong Sag, Bohai Bay Basin, East China. *Pet. Explor. Dev.* **2022**, *49*, 1107–1118. [CrossRef]
16. Luo, J.; Morad, S.; Liang, Z.; Zhu, Y. Controls on the quality of Archean metamorphic and Jurassic volcanic reservoir rocks from the Xinglongtai buried hill, western depression of Liaohe basin, China. *AAPG Bull.* **2005**, *89*, 1319–1346. [CrossRef]
17. Maryi, R.; Agustín, C.; Gaspar, M.; Sebastián, Z.; Juan, C. Fracture evaluation of the plutonic basement in the Upper Magdalena Basin: Implications for the development of naturally fractured reservoirs in the Northern Andes. *Wiley* **2024**, *59*, 1968–1997.
18. Zhao, X.; Jin, F.; Wang, Q.; Bai, G. Buried-hill play, Jizhong subbasin, Bohai Bay basin: A review and future prospectivity. *AAPG Bull.* **2015**, *99*, 1–26. [CrossRef]
19. Dong, G.; He, Y. Mechanism of sand body prediction in a continental rift basin by coupling paleogeomorphic elements under the control of base level. *Pet. Explor. Dev.* **2016**, *43*, 529–539. [CrossRef]
20. Li, C.; Yang, X.; Fan, C.; Hu, L.; Dai, L.; Zhao, S. On the Evolution Process of the Beibu Gulf Basin and Forming Mechanism of Local Structures. *Acta Geol. Sin.* **2018**, *92*, 2028–2039.
21. Li, W.; Liu, C.; Zhang, J.; Duan, J.; Chen, W.; Chen, X. Structure physical modeling experiment of evolutionary mechanism about fault system in eastern area of Maichen sag, Beibu-gulf Basin. *J. China Univ. Pet.* **2015**, *39*, 38–46.
22. Deng, Y.; Hu, D.; Zhu, J.; Liu, G.; Chen, K.; Tong, C. Hydrocarbon accumulation regularities, new fields and new types of exploration, and resource potentials in Beibuwan Basin. *Acta Pet. Sin.* **2024**, *45*, 202–225.
23. Xing, Y. A Study of carbonate paleo buried hill reservoir in Beibu Gulf W10-3N field. *Pet. Explor. Dev.* **1993**, *20*, 100–108.
24. Zhao, S.; Zhao, Y.; Yang, X.; Jiao, L.; Chen, C. An analysis on the characteristics and main controlling factors of reservoir in carbonate buried hill in the Weixi'nan Sag, Beibuwan Basin. *Haiyang Xuebao* **2018**, *40*, 43–53.
25. Xu, G.; Chen, F.; Zhou, X.; Wang, X.; Li, J.; Wang, X. Hydrocarbon accumulation process of large scale oil and gas field of granite buried hill in Penglai 9 1 structure, Bohai, China. *J. Chengdu Univ. Technol.* **2016**, *43*, 153–162.
26. Liu, Z.; Zhu, M.; Liu, H.; Li, X.; Liang, S.; Gong, J. Formation mechanism and distribution characteristics of granitic weathering crust reservoir: A case study of the western segment of the northern belt of Dongying sag. *Acta Geol. Sin.* **2021**, *42*, 163–175.
27. Tari, G.; Connors, C.; Flinch, J.; Granath, J.; Pace, P.; Sobornov, K. Negative structural inversion: An overview. *Mar. Pet. Geol.* **2023**, *152*, 106223. [CrossRef]
28. Bonini, M.; Sani, F.; Antonielli, B. Basin inversion and contractional reactivation of inherited normal faults: A review based on previous and new experimental models. *Tectonophysics* **2012**, *522*, 55–88. [CrossRef]
29. Faccenna, C.; Nalpas, T.; Brun, J.; Davy, P. The influence of pre-existing thrust faults on normal fault geometry in nature and in experiments. *Pergamon* **1995**, *17*, 1139–1149. [CrossRef]
30. Nicola, D.; Nicolas, C.; Renato, F.; Laurent, J.; Fabio, S. The role of pre-existing thrust faults and topography on the styles of extension in the Gran Sasso range (central Italy). *Tectonophysics* **1998**, *292*, 229–254. [CrossRef]
31. Liu, J.; Xia, B.; Lv, B.; Cai, Z.; Shi, Q.; Yuan, Y. Comparative Analysis of Inversion Structure with Its Easily Confused Structures. *Geoscience* **2010**, *24*, 744–748.
32. Xu, C.; Peng, J.; Wu, Q.; Sun, Z.; Ye, T. Vertical dominant migration channel and hydrocarbon migration in complex fault zone, Bohai Bay sag, China. *Pet. Explor. Dev.* **2019**, *46*, 684–692. [CrossRef]
33. Huang, B.; Tian, H.; Wilkins, R.; Xiao, X.; Li, L. Geochemical characteristics, palaeoenvironment and formation model of Eocene organic-rich shales in the Beibuwan Basin, South China Sea. *Mar. Pet. Geol.* **2013**, *48*, 77–89. [CrossRef]
34. Xie, B.; Xu, F.; Fan, C.; Man, Y.; Jiang, F.; Xu, G. Karst Identification and Development Model of Buried Hill Limestone Reservoir in Weixinan Depression, Beibuwan Basin. *J. Jilin Univ.* **2024**, *54*, 2029–2046.
35. Hua, W.; Guo, F.; Wen, Y.; Zhao, L. Caledonian subduction of Proto-Tethyan Ocean beneath the Yunkai Massif: Petrological and geochemical evidence from Late Ordovician mafic intrusions. *Acta Petrol. Sin.* **2024**, *40*, 2469–2488. [CrossRef]
36. Liu, S. Origin and tectonic implications of an Early Paleozoic tectonic mélange in the northwestern Yunkai Domain, South China. Ph.D. Dissertation, China University of Geosciences, Wuhan, China, 2018.
37. Wang, Y.; Zhang, A.; Fan, W.; Zhang, Y.; Zhang, Y. Origin of paleosubduction-modified mantle for Silurian gabbro in the Cathaysia Block: Geochronological and geochemical evidence. *Lithos* **2013**, *160*, 37–54. [CrossRef]
38. Ventisette, C.; Montanari, D.; Bonini, M.; Sani, F. Positive fault inversion triggering 'intrusive diapirism': An analogue modelling perspective. *Terra Nova* **2005**, *17*, 478–485. [CrossRef]
39. Li, C.; Fan, C.; Hu, L.; Hu, Q.; Chen, L. Tectonic evolution characteristics and genesis of Weixi'nan low uplift in Beibu Gulf Basin. *Mar. Orig. Pet. Geol.* **2021**, *26*, 319–325.
40. Gao, G.; Xu, X.; Liu, S.; Gan, J.; Hu, C.; Zhao, J. Organic geochemistry identification of high-quality source rocks in the 2nd member of Liushagang Fm and its controls on petroleum occurrence in the Weixi'nan Sag, Beibuwan Basin. *Oil Gas Geol.* **2020**, *41*, 339–347.
41. Burton, Z.F.M.; McHargue, T.R.; Kremer, C.H.; Bloch, R.B.; Gooley, J.T.; Jaikla, C.; Harrington, J.; Graham, S.A. Peak Cenozoic warmth enabled deep-sea sand deposition. *Sci. Rep.* **2023**, *13*, 1276. [CrossRef]

42. Burton, Z.F.M.; McHargue, T.R.; Graham, S.A. Global Eocene-Oligocene unconformity in clastic sedimentary basins. *Earth-Sci. Rev.* **2024**, *258*, 104912. [CrossRef]
43. Huang, B.; Zhu, W.; Tian, H.; Jin, Q.; Xiao, X.; Hu, C. Characterization of Eocene lacustrine source rocks and their oils in the Beibuwan Basin, offshore South China Sea. *AAPG Bull.* **2017**, *101*, 1395–1423. [CrossRef]
44. Gan, H.; Wang, H.; Shi, Y.; Ma, Q.; Liu, E.; Yan, D. Geochemical characteristics and genetic origin of crude oil in the Fushan sag, Beibuwan Basin, South China Sea. *Mar. Pet. Geol.* **2020**, *112*, 104114. [CrossRef]
45. Passey, Q.R.; Bohacs, K.M.; Esch, W.L.; Klimentidis, R.; Sinha, S. From oil-prone source rock to gas-producing shale reservoir -Geologic and petrophysical characterization of unconventional shale-gas reservoirs. In Proceedings of the SPE International Oil and Gas Conference and Exhibitionin China, Beijing, China, 8–10 June 2010; Society of Petroleum Engineers: Houston, TX, USA, 2010; p. SPE-131350-MS.
46. Burton, Z.F.M.; Dafov, L.N. Testing the sediment organic contents required for biogenic gas hydrate formation: Insights from synthetic 3-D basin and hydrocarbon system modelling. *Fuels* **2022**, *3*, 555–562. [CrossRef]
47. Xiao, W.; Cao, J.; Luo, B.; Wang, Y.; Xiao, D.; Shi, C.; Hu, K. Recovering original type and abundance of organic matter in spent source rocks: A review and advances in elemental proxies. *AAPG Bull.* **2023**, *107*, 243–281. [CrossRef]
48. Peters, K.E.; Cassa, M.R. Applied source rock geochemistry. In *The Petroleum System—From Source to Trap; American Association of Petroleum Geologists Memoir 60*; Magoon, L.B., Dow, W.G., Eds.; American Association of Petroleum Geologists: Tulsa, Oklahoma, 1994.
49. Peters, K.E. Guidelines for evaluating petroleum source rock using programmed pyrolysis. *AAPG Bull.* **1986**, *70*, 318–329. [CrossRef]
50. Gratzer, R.; Bechtel, A.; Sachsenhofer, R.F.; Linzer, H.G.; Reischenbacher, D.; Schulz, H.M. Oil-oil and oil-source rock correlations in the Alpine Foreland Basin of Austria: Insightsfrom biomarker and stable carbon isotope studies. *Mar. Pet. Geol.* **2011**, *28*, 1171–1186. [CrossRef]
51. Burton, Z.; Moldowan, J.M.; Sykes, R.; Graham, S.A. Unraveling petroleum degradation, maturity, and mixing and addressing impact on petroleum prospectivity: Insights from frontier exploration regions in New Zealand. *EnergyFuels* **2018**, *32*, 1287–1296. [CrossRef]
52. Yelwa, N.A.; Mustapha, K.A.; Opuwari, M.; Aziz, A.A. Biomarkers, stable carbon isotope, and trace element distribution of source rocks in the Orange Basin, South Africa: Implications for paleoenvironmental reconstruction, provenance, and tectonic setting. *J. Pet. Explor. Prod. Technol.* **2022**, *12*, 307–339. [CrossRef]
53. Peters, K.E.; Walters, C.C.; Moldowan, J.M. *The Biomarker Guide*; Cambridge University Press: Oxford, UK, 2005.
54. He, M.; Moldowan, J.M.; Peters, K.E. Biomarkers: Petroleum. In *Encyclopedia of Geochemistry*; Springer: Cham, Switzerland, 2018.
55. Burton, Z.; Moldowan, J.M.; Magoon, L.B.; Sykes, R.; Graham, S.A. Interpretation of source rock depositional environment and age from seep oil, east coast of New Zealand. *Int. J. EarthSciences* **2019**, *108*, 1079–1091.
56. Walters, C.C.; Peters, K.E.; Moldowan, J.M. History of life from the hydrocarbon fossil record. In *Hydrocarbons, Oils and Lipids: Diversity, Origin, Chemistry and Fate*; Springer: Cham, Switzerland, 2020.
57. Li, Y.; Lan, L.; Wang, K.; Yang, Y. Differences in lacustrine source rocks of Liushagang Formation in the Beibuwan Basin. *Acta Pet. Sin.* **2019**, *40*, 1451–1459.
58. Zhao, S.; Yang, X.; Chen, L.; Zhou, G.; Jiao, L.; Zhao, Y. Hydrocarbon accumulation conditions and exploration potential of carbonate buried hills in Weixinan sag in western South China Sea. *China Offshore Oil Gas* **2019**, *31*, 51–61.
59. Ma, Q.; Zhao, S.; Liao, Y.; Lin, Z. Sequence Architectures of Paleogene Liushagang Formation and Its Significance in Fushan Sag of the Beibuwan Basin. *Earth Sci. J. China Univ. Geosci.* **2012**, *37*, 667–678.
60. Yu, S.; Deng, Y.; Li, H.; Xiao, L.; Wu, A.; Li, F.; Zhang, Z. Forming conditionsand distribution controlling factors of oil shale in Liu 2 Memberof Beibuwan Basin. *China Offshore Oil Gas* **2020**, *32*, 24–33.

Disclaimer/Publisher's Note: The statements, opinions and data contained in all publications are solely those of the individual author(s) and contributor(s) and not of MDPI and/or the editor(s). MDPI and/or the editor(s) disclaim responsibility for any injury to people or property resulting from any ideas, methods, instructions or products referred to in the content.